Transformation of Wave Spectra across a Line of Wave Devices

A. Alexandre, T. Stallard and P.K. Stansby[1]

[1]Joule Centre, School of Mechanical, Aerospace and Civil Engineering,
The University of Manchester,
PO Box 88, M60 1QD, Manchester, UK
E-mail: Armando.Alexandre@postgrad.manchester.ac.uk

Abstract

As the deployment scale of wave farms increases towards hundreds of MW installed capacity, it becomes important to understand how nearshore coastal processes may be modified by energy extraction. Most of the published studies on the environmental impact of wave energy converters represent a group of devices using transmission and absorption coefficients. This approach represents the average energy extraction across the power spectrum but, since wave device performance is dependent on the wave frequency, the use of frequency-dependent transmission coefficients may be more appropriate. In this study, SWAN is used to investigate how the definition of a frequency-dependent transmission coefficient, based on an idealised point absorber, alters nearshore conditions relative to a constant transmission coefficient. Experimental measurements are also presented to quantify the change of wave characteristics due to a small array of heaving point absorbers. Wave spectra measured down-wave and up-wave of arrays comprising five- and ten- devices are compared to those measured at the same location prior to device deployment. The influence of these modifications on breaking conditions near the shoreline is briefly discussed and the measurements provide the basis for evaluation of numerical models of device arrays at the site scale.

Keywords: Spectrum changes, WEC, Nearshore

Nomenclature

a	=	float radius
c	=	wave velocity
d	=	water depth
H	=	wave height
F	=	Force
f	=	frequency
I	=	electric current
N	=	action density
P	=	power
q	=	SWAN parameter
r	=	SWAN parameter
S	=	source term
T	=	wave period
WEC	=	wave energy converter
x, y	=	cartesian co-ordinate system
β	=	seabed slope angle
δ	=	damping coefficient
ω	=	angular frequency
θ	=	wave direction
σ	=	relative frequency

Subscripts

a	=	Absorbed
e	=	excitation
g	=	group
0	=	natural frequency
p	=	peak
max	=	maximum
min	=	minimum
s	=	significant
t	=	time
x	=	tangential component
y	=	axial component
ξ	=	streamwise component
η	=	normal to the streamwise direction

1 Introduction

During the last few years several wave energy devices have been demonstrated offshore and one demonstrator array has been installed in Portugal. It is well-known that commercial scale projects will comprise large arrays of small capacity devices and so it is increasingly important to understand the environmental effects due to these schemes. In particular, changes to the nearshore wave conditions can influence several coastal processes. Large changes of breaking wave height, particularly during storm conditions, will alter erosion patterns. Even apparently small changes of the breaking wave height or location may result in changes to longshore currents or sediment transport and so may have longer term environmental implications. Initial studies of device performance indicate that two lines of optimal wave energy devices could completely eliminate the incoming wave [1]. The performance of real devices is

© Proceedings of the 8th European Wave and Tidal Energy Conference, Uppsala, Sweden, 2009

somewhat less impressive and tends to vary with incident wave conditions. Within the process of harvesting energy from the waves, devices interact with the waves, and this changes the wave field near the wave energy devices. The incident waves are going to be scattered by the presence of the wave energy device structure in the water. Besides this process, the displacement of the device is also going to generate waves, radiated waves. The wave which is going to propagate to the coast is going to be the sum of all these components: the incoming wave, scattered wave and waves radiated by the WEC.

Although much of the literature on wave energy concerns device development, a small number of studies have been published concerning the change of shoreline wave conditions due to wave device deployment. These have mostly focused on particular test-sites in locations such as Scotland, Cornwall, Spain and Portugal. All these studies have shown, in different magnitudes, that energy extraction has some influence on nearshore wave conditions. One of the earliest studies addressed the impact of a proposed wave farm in the South West of England: the Wave Hub [2]. Their study was based on the use of a 4 km wave farm, implemented in the wave propagation model through a energy transmission coefficient. Related with this project also some initial studies using the near shore simulation code SWAN and several sensitivity studies [3]. The wave climate near an array of wave energy devices was also investigated using Boussinesq equations in the code MIKE21 [4]. The array was modelled as a fixed structure in the seabed and different energy transmission coefficients were used by defining an appropriate structure porosity. A similar study was completed for Santana, North of Spain with the implementation of 10 wave energy devices of 125kW each [5]. The interaction of the WEC array with the waves was based on the energy production of a device, and a transmission coefficient reducing the energy of the waves at the location of the farm. A similar study for a future wave device deployment zone in the Atlantic Coast of Portugal has also been presented [6] using the computer code REF-DIF and transmission coefficients to represent energy extraction by wave energy devices.

A common feature of all these studies is that the interactions between each wave energy conversion device (or group of devices) is not explicitly modelled. Instead, the effect of devices is modelled using frequency independent transmission coefficients, i.e. the ratio of the significant wave height, H_s, before and after the array [7]. Since the power output of nearly all wave devices is dependent on the frequency of the incident wave conditions, this is a poor representation of the process. For a device that is optimised for operation in a particular sea-state (i.e. natural frequency similar to peak frequency, f_p), energy reduction would only occur over a frequency range close to the peak frequency. There would be little change to low or high frequency components but the central range is reduced. In the limit case of 100% energy extraction at the peak frequency, a single-peaked incident wave spectrum would be transformed to a bi-modal spectrum inshore. During propagation to the shoreline, a bi-modal spectrum would be subject to different losses to a single-peaked spectrum with the same energy content. Energy content would be higher at either end of the spectrum and so energy dissipation due to bed-friction (long period waves) and whitecapping (short period waves) would be greater for a bi-modal spectrum. Even though the resultant changes to the averaged characteristics of the spectrum may not differ greatly for these two cases, the changes to the nearshore wave spectra may alter nearshore processes.

In this paper a study of the different processes that are not accounted for in the frequency independent characterisation is presented. In Section 2, the nearshore wave model SWAN is used to compare the onshore propagation of an idealised Bretschneider spectra due to a frequency-independent and frequency-dependent transmission coefficient. Frequency-dependent cases are based on an idealised device tuned to the sea-state and on experimental measurements of the wavefield changes in the vicinity of a line of heaving point absorbers. This is clearly an idealisation and so experimental measurements are also presented in Section 3 of the change of wave spectra due to several small arrays of devices. Nearshore propagation of the transmitted waves reported in Section 4 is also discussed.

2 Wave Propagation Model - SWAN

The wave propagation model used for this study was SWAN - Simulation WAves Nearshore[8]. SWAN is third generation wave spectral propagation model; a phase averaged action density balance equation solver. The action (N) balance equation, Equation 1, is mainly the energy balance, however due to the possible presence of currents the frequency used is a relative frequency (σ) to account for possible change of the group speed (c_g). Zero current is specified in all simulations presented here, the relative frequency, σ can however be transformed to absolute frequency, f using a transfer function available in SWAN [7].

$$\begin{aligned} \frac{S(\sigma,\theta,x,y,t)}{\sigma} &= \frac{\partial N(\sigma,\theta,x,y,t)}{\partial t} \\ &+ \frac{\partial c_{g,x} N(\sigma,\theta,x,y,t)}{\partial x} + \frac{\partial c_{g,y} N(\sigma,x,y,t)}{\partial y} + \\ &+ \frac{\partial c_{g,\theta} N(\sigma,\theta,x,y,t)}{\partial \theta} + \frac{\partial c_{\sigma} N(\sigma,\theta,x,y,t)}{\partial \sigma} \end{aligned} \tag{1}$$

The method used is based on the integration of the action density using finite differences in time (t), geographic space (spatial co-ordinates x, y), and spectral space (heading θ and frequency σ). SWAN uses a constant time step for the propagation and integration [8]. SWAN also accounts for some physical phenomena present in the ocean including wind growth by the source term S in Equation 1, dissipation processes and wave-wave interactions. The dissipation mechanisms present in the model are bottom friction, whitecapping and depth induced breaking.

The bottom friction in the model represents energy losses in the waves originated by the processes in the seabed. The amount of energy dissipated with bottom friction, besides depending on several calibration factors for different type of seabed, depends on the particle velocity at the seabed [9]. Hence in irregular waves, this process is expected to be more important for low frequencies as higher bed-velocities are expected in longer waves. Losses of energy originated by the whitecapping represent the spilling of some waves in deep water. It is a very complex process relating capillary waves, non-linear interaction and turbulence components. SWAN uses a pulse-based model [10] where the energy dissipated depends on the overall steepness of the spectrum and on wave frequency. So it is expected to be a more relevant process for high frequency waves. The depth induced wave breaking in SWAN is implemented using the bore-based model [11]. The energy dissipation is dependent on the fraction of breaking waves, the maximum wave height for a particular depth and the mean frequency. This reduction is expected to occur in a frequency independent fashion along the spectrum.

SWAN also accounts for energy shifting mechanisms. There are the fourth order wave-wave interactions more important in deep water, QUADRUPLETS only modelled in SWAN correctly when wind growth waves are present. Also, and more important for this study, TRIADS, third order interaction models important for shallow and intermediate waters. TRIADS represent energy shifting from lower frequencies to higher frequencies; hence new peaks develop in the wave spectrum at higher frequencies as a wavefield propagates into shallow water. SWAN uses the Lumped Triad Approximation (LTA) [12] for modelling this phenomena. The development of higher frequency spectral peaks could lead to steeper waves in nearshore waters and so the wave breaking phenomena could be more significant. Observations have shown that the new formed peaks will tend to disappear in further shallow waters [13]. The LTA model implemented in SWAN does not account for these further changes. However, the LTA model has been validated against experimental measurements from a unidirectional wave flume with satisfactory results [8].

To understand how wave energy extraction may influence the relative importance of the main energy dissipation mechanisms, an idealised model is employed. The relative captured power by an axisymmetric point absorber with optimal power captured, P_a for different frequencies can be defined by Equation 2 [14]. This definition can then be applied to the incoming spectrum, and the power absorbed by an optimal device calculated.

$$\frac{P_a(\omega)/|\hat{F}_e(\omega)|^2}{P_a(\omega_0)/|\hat{F}_e(\omega_0)|^2} = \frac{1}{1+(\omega_0/\delta)^2(\omega/\omega_0-\omega_0/\omega)^2} \tag{2}$$

Where $\hat{F}_e$ is the excitation force on the stationary immersed geometry due to the diffracted wave-field, ω the angular frequency of the incident wave, ω_0 the resonance frequency of the device and δ the damping coefficient of the oscillator. The device considered is tuned such that the natural frequency is the same as the peak frequency of the incoming spectrum. The WEC is considered able to convert 75 % of the incoming wave energy. The initial wave field is described by a Bretschneider spectrum with H_s=2.7 m and T_p=10.7 s. The subtraction of the power extracted from this optimal device at different frequencies and the incoming spectrum it's considered the resultant spectrum that will propagate to the shore. In Figure 1 the resultant bi-modal spectrum considered for the model with the WEC is shown as line 3. The simple subtraction of the power spectrum for the device from the incident Bretschneider spectrum is not the ideal representation of the WEC array interactions with the wave field. There will be other phenomena involved, for example, neither the scattered or radiated wavefields are accounted for here. Nevertheless, it is an improved representation compared with the use of a simple transmission coefficient for WEC modelling. For comparison, another spectrum is also considered based on the transmission factor definition. This is an equivalent spectrum with the same energy extracted as the optimal device, however this energy is now extracted in all the frequencies at the same rate hence forming a single peak spectrum (line 4 in Figure 1). This is the same type of approach used in most of the wave farm impact studies, the use of a constant transmission coefficient defined as a H_s ratio before and after the array.

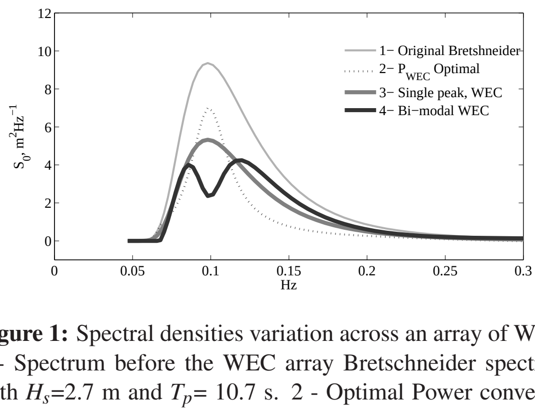

Figure 1: Spectral densities variation across an array of WEC. 1 - Spectrum before the WEC array Bretschneider spectrum with H_s=2.7 m and T_p= 10.7 s. 2 - Optimal Power converted by a WEC, corresponding to 75% of the incoming power. 3 - Resultant wave spectrum.4- Constant transmission spectrum

A 1-D SWAN model is employed with a sloping bed of horizontal length 3000 m from the outer boundary to the beach. A constant sea bed gradient of 1% is employed and the device is assumed to be coincident with the outer boundary at a water depth of 30 m, Figure 2. The dissipation mechanisms considered in the propagation model were: bottom friction (with JONSWAP friction coefficient of $0.067 \mathrm{m}^2\mathrm{s}^{-2}$, $q = 1$ and $r = 4$ [7]), whitecapping (steepness dependent coefficient equals to 2.36×10^{-5} and $q = 1$ and $r = 4$ [7]) and wave breaking due to depth (ratio of maximum individual wave height over depth equals to 0.73 [7]). Non-linear wave-wave interactions were also considered with the inclusion of the TRIADS mechanism, more relevant for nearshore cases. The spatial grid used had cells with 15 m long, and frequency range of 0.05 to 0.6 Hz with 75 intervals considered.

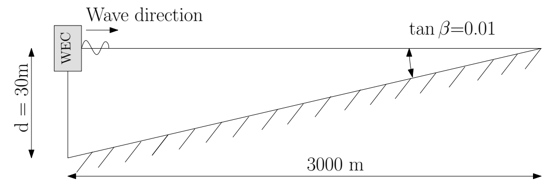

Figure 2: Model used for wave propagation .

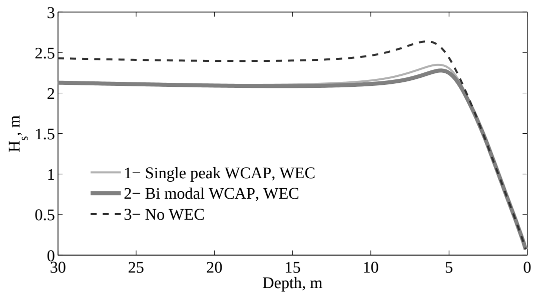

Figure 3: H_s variation with water depth for different initial spectrum definitions: **1-** With WEC array originating a single peak wave spectrum, **2-** WEC array with bi-modal initial spectrum, **3-** No WEC, original incident spectrum.

The differences on the wave propagation to the shoreline are well defined in terms of H_s. The energy extracted by the device, corresponds to a 25% decrease of H_s at the initial point in deep water. By definition, the H_s value for the initial point are the same for both of the idealised devices. However as the wave propagates into shallower water the differences between the two cases are noticeable, not only in terms of H_s but also in terms of spectrum evolutions, as can be seen in Figure 4. From the deeper case ($d = 30$ m, upper figure) and intermediate case ($d = 10$ m, middle figure) before the wave breaking zone it can be seen that the characteristics of the two spectra are maintained, so the predominance of high frequencies in the bi-modal spectrum is preserved. This also indicates that average wave group velocity is smaller in the bi-modal spectrum than in the single peak spectrum, Figure 5. This implies that the energy transmitted by the bi-modal spectrum can be smaller than that of the single peak spectrum and this is shown in Figure 6. Since both spectra are defined with the same transmission coefficient, the energy of both is the same but the bi-modal spectrum has a lower group velocity since the average frequency of the spectrum is higher.

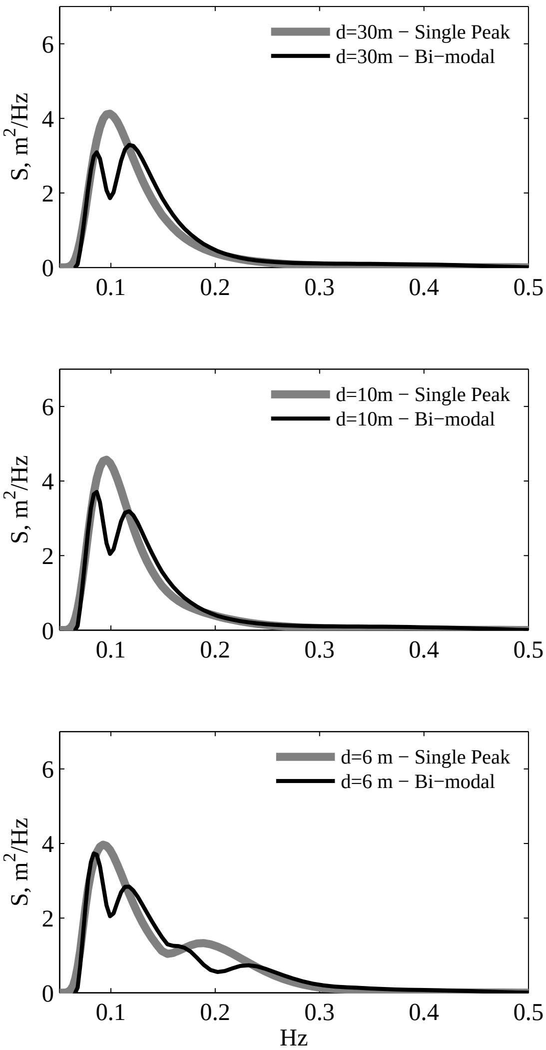

Figure 4: Spectral density evolution for 3 water depths: 30, 10 and 6 m, for the cases with WEC. **1-**Single peak spectrum, **2-** Bi-modal spectrum.

From Figure 6 it can be seen that the quantity of transported energy decreases with water depth. This is caused by the three energy dissipation mechanisms included in the model. Besides the energy lost in the wave breaking regions ($d < 6$ m) not much more information about the dissipation processes can be extracted from this figure. In order to understand the differences between the two spectra definitions on nearshore wave conditions it is informative to consider how the wave spectra changes due to energy dissipation in the region between offshore ($d = 30$ m) and the breaking zone. In this region, the other processes considered before the wave breaking assume more importance; these are bottom friction and whitecapping. The cumulative loss of energy with distance to shore is shown for the

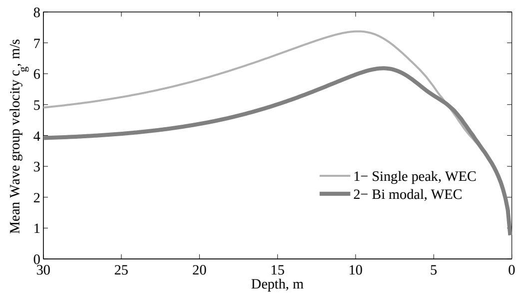

Figure 5: Averaged wave group velocity for different locations .**1-**Single peak spectrum, **2-** Bi-modal spectrum.

dissipated energy with bottom friction and whitecapping in Figures 7(b) and 7(c), respectively. The two different spectra will have different behaviours as far as whitecapping and bottom friction is concerned since both processes are dependent on wave frequency. For bottom friction it can be seen that with the single peak spectrum a large amount of energy is dissipated in all the points of the domain. As described in Section 2, bottom friction is a phenomenon that depends on the horizontal velocity of particles at the bed and the predominance of lower frequencies in this spectrum will originate larger losses due to bottom friction. The whitecapping depends on the wave steepness. The bi-modal spectrum presents a higher frequency characteristic, hence the losses due to the whitecapping phenomena for this spectrum are higher at all locations along the domain than for the single peak spectrum.

The interconnection of these processes and the regions over which they occur is also important in terms of energy dissipated in the breaking zone. For example, if a high frequency dominated spectrum propagates to the coast, energy will primarily be dissipated by whitecapping, which can then change the spectrum shape, hence the propagation velocities. As a result dissipation through bottom friction can increase and so different behaviour in the breaking zone may be expected. By extracting energy from only finite frequency ranges of a wave spectrum, the relative importance of natural energy dissipation mechanisms clearly changes.

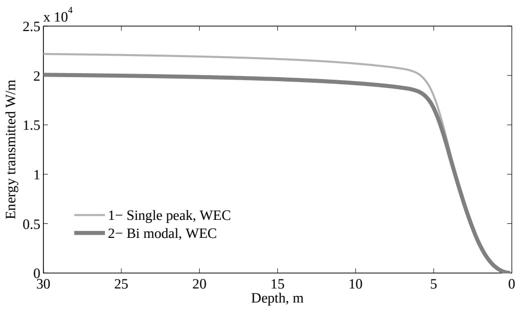

Figure 6: Wave Energy transported in the different depths. Comparing the **1-** With WEC array originating a single peak wave spectrum, **2-** WEC array with bi-modal initial spectrum. –Changed the linestyle

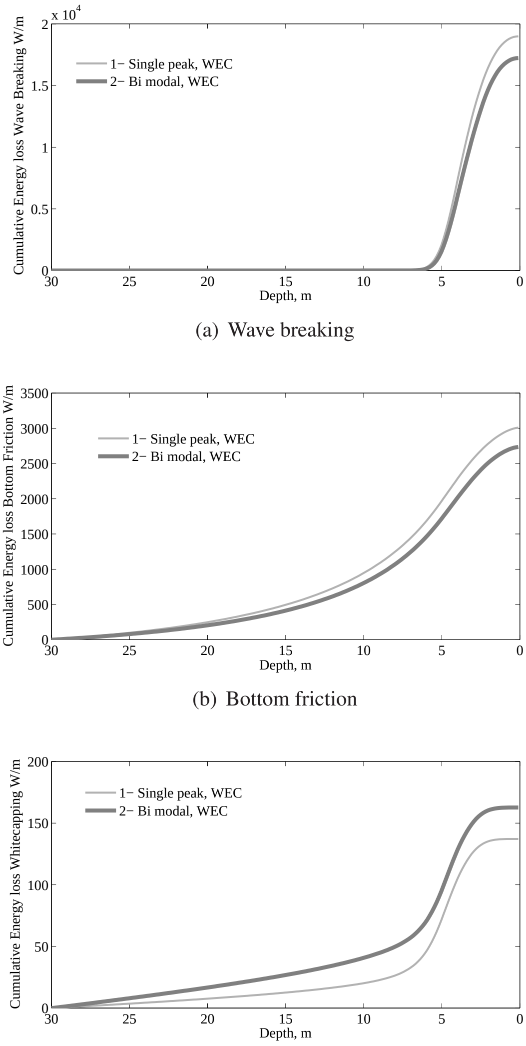

(a) Wave breaking

(b) Bottom friction

(c) Whitecapping

Figure 7: Cumulative energy dissipated in **a)** Wave breaking, **b)** Bottom friction and **c)** Whitecapping. Comparing the **1-** With WEC array originating a single peak wave spectrum, **2-** WEC array with bi-modal initial spectrum.

With this analysis it can be seen that the two initial representations for the WEC spectrum will originate the same value of H_s in offshore waters but H_s differs slightly (by 5%) as the spectrum propagates towards the shoreline (Figure 3). The breaking location does seem not to change significantly. This first approach was based on an idealised model of the energy extraction due to a wave energy converter. When real devices are used the spectral response is expected to be different. An approach for obtaining spectral changes based on the linear hydrodynamic parameters of a given immersed geometry is described in [15]. Actual WEC deployments are likely to be in arrays. The wavefield transmitted across an array is also different from a single WEC due to the radiated and scattered waves from each device interacting with the remaining devices. Hence the representation of spectrum changes due to real, and particularly closely spaced, arrays based on linear wave models alone is a complex process. In the following

Section, a first approximation for the resultant wave fields across an array of devices was done with some experiments in a wave tank measuring the wave field before and after a WEC array.

3 Experimental Measurements

In this study experimental measurements of the transformation of an irregular wave-field in the vicinity of an array of wave devices are presented and discussed. The wave energy converter used for this was the Manchester Bobber, a heaving point absorber. Each full-scale device comprises a 10 m diameter float whose motion drives a generator rated at between 300 and 600kW. Experiments were conducted at 1:67th geometric scale in the University of Manchester wide flume (5 m wide, 18.5 m long, 0.45 m deep) with the generator modelled using a friction-compensated dynamometer. Each device consists of a float (7.5 cm radius and 1.8 kg mass) partially supported by a counterweight (0.4 kg) and whose vertical oscillation is translated into flywheel rotation via a pulley and clutch. Electricity is generated from the unidirectional rotation of the fly-wheel using an induction generator and the torque-speed curve of this machine is reproduced at model scale using a calibrated dynamometer. The torque-speed curve is specified for the device in terms of the maximum current to be drawn by the generator, I_{max}. To avoid stall, actual current extracted from the generator is linear with the pulley rotational speed (ω) for low ω, after a certain value ω_{min} the set value for maximum current is used and the maximum power for that configuration produced. More details on the device used for these tests are presented in [16, 17]. One of the main features of this device is the configuration of the floats at close spacing of the order of two diameters. Here, two array configurations are considered: a single row of 5 devices normal to the direction of wave propagation (termed 5 $\times$ 1) and a double row of 5 devices (termed 5 $\times$ 2). The load applied by each dynamometer is specified to represent full-scale power outputs equivalent to 300 kW and 600 kW per device, corresponding to normal operating conditions. Irregular waves were defined according to a Bretschneider Spectrum for a 2.7 m significant wave height (H_s) and 10.7 s. peak period (T_p) using the Edinburgh Designs OCEAN software [18]. The wave-field was measured pre- and post- deployment at two lines of three wave gauges up- and down-wave of the array to quantify the change of wave spectrum. In Figure 8 the set up used for the experiments is shown.

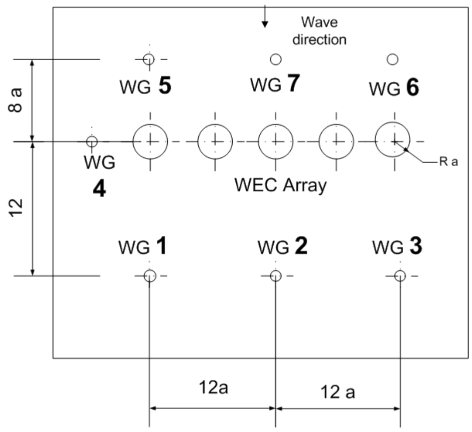

Figure 8: Experimental set up used. *a* is the radius of the floats = 7.5 cm.

3.1 H_s Changes

The experimental results presented in Figure 9 indicate the reduction of the significant wave height, H_s, across the array in all cases tested. A maximum 14% H_s reduction is measured across the centreline of the array when the 5 $\times$ 2 array was in use. The results were obtained taking into account the modifications in the waves pre and post WEC array deployment. As would be expected, a larger reduction is observed across the centreline of the array since the array is symmetric upwave of this location. These changes of significant wave height represent the net change of wave conditions due to wave scattering and radiation by the array and are comparable to an absorption coefficient. The magnitude of the reduction clearly varies with both the number and rated-power of the devices installed. For the 5×2 configuration a reduction of H_s is observed at the centreline and one side of the array as the rating is increased from 300kW to 600kW. In this case, power output per device was slightly asymmetric and the resultant change of wave heights is also asymmetric. However, for the 5×1, an increase of rated power results in a smaller reduction of wave height ($\sim$ 2%) across the array. The measured power from the 5x1 configuration is 75kW when rated at 600kW and 56 kW when rated at 300kW and so energy extraction is greater despite this smaller change of wave height. This perhaps occurs since the float motion is reduced at higher rated power and so the radiated wave field is of smaller amplitude.

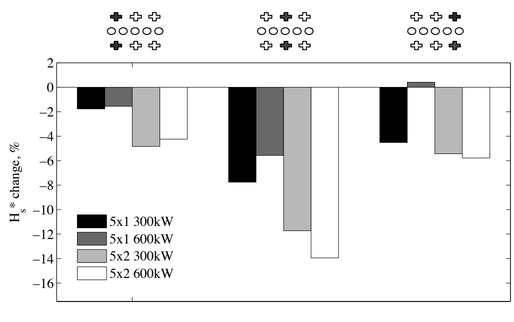

Figure 9: H_s across the devices array for 3 different rows of wave gauges, using a Bretschneider spectrum of $T_p = 10.7$s and $H_s = 2.67$m extracting 300 kW and 600 kW per device.

3.2 S_0 Changes

In Figures 10 and 11 the values for the spectral density variation across a WEC array are presented for two specific locations, one in an up wave location, and other in a downwave location pre and post the deployment of the WEC array (WG7 and WG2 in Figure 8). The considered array was the 5×2 case with power extraction of 600 kW. Spectra were obtained by Fourier analysis of the measured time-varying water surface elevation. The change of wave spectrum at an upwave position is shown in Figure 10. WEC installation reduces wave energy slightly near the peak frequency of the spectrum although increased energy content is observed over other frequency ranges. This is explained due to the waves radiated by the devices in the array have a radial pattern and some of the incident waves are also reflected by the WEC. The downwave location, Figure 11 indicated that the array changes the wave spectrum in different forms in a frequency dependent fashion. The main energy reductions occur in two distinct regions: near the peak frequencies, with a energy reduction near 30%, the other region is located on the natural frequency of the devices used, at frequencies around 0.15 Hz.

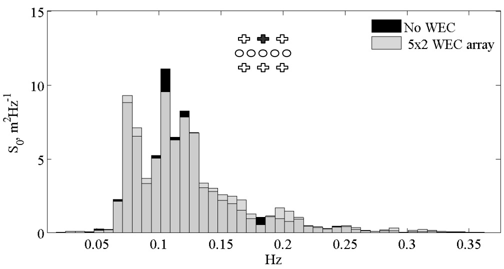

Figure 10: Changes in the wave spectrum before the WEC array, pre and post WEC deployment. Using a Bretschneider spectrum of $T_p = 10.7s$ and around $H_s = 2.7m$ and extracting approximately 600 kW each device using an 5×2 array .

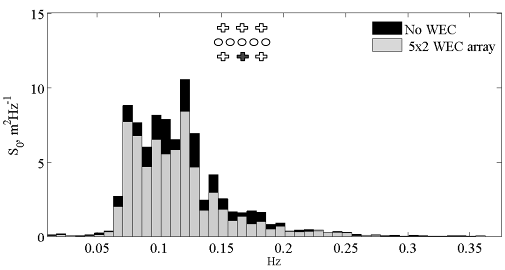

Figure 11: Changes in the wave spectrum after the WEC array, pre and post WEC deployment. Using a Bretschneider spectrum of $T_p = 10.7s$ and around $H_s = 2.7m$ and extracting approximately 600 kW each device using an 5×2 array.

4 Wave Propagation after WEC arrays

Although preliminary at this stage, these experimental measurements indicate that the transfer from incident to transmitted spectrum varies significantly with component wave frequency. As seen in Figure 1 the WEC array considered does not extract power in the same fashion for the different zones of the incident wave spectrum. Usually devices are tuned in order to have their peak of power absorption near the peak frequency of the incoming spectrum. The point absorbers used in this experiment have a similar behaviour. Moreover the fact of the devices being incorporated in an array will also change the devices responses, as the scattered and radiated waves are going to interact and change the incoming wave to the devices. To understand the influence of these frequency-dependent spectral changes on nearshore wave conditions, similar spectral changes were implemented in the SWAN wave model. The model used was the same as the one described in Section 1 where a location 3000 m from the coast is chosen with water depths of 30 m, and a constant sea bed slope until the beach, Figure 2. The dissipation processes considered were: the depth induced wave breaking, whitecapping and bottom friction. The wave-wave interactions considered were the TRIADS, which are the more relevant in nearshore waters. As considered in the initial study with the optimal device a spectrum corresponding to a constant transmission factor for all frequencies (corresponding to the measured H_s reduction) was also considered. Since the experimental measurements do not accurately represent the shape of a Bretschneider spectrum (Figure 11), the measured percentage changes were instead applied to a Bretschneider spectrum to provide a new spectrum, curve 3 of Figure 12.

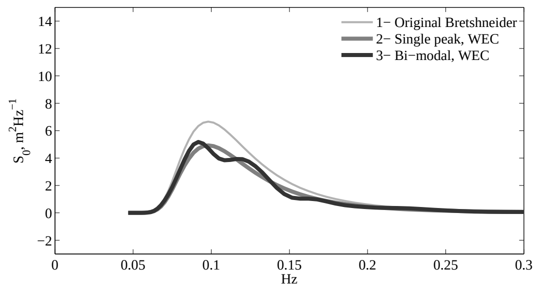

Figure 12: Spectral densities variation across an array of WEC. **1-** No WEC, original incident spectrum.**2-** With WEC array originating a single peak wave spectrum, **3-** WEC array with bi-modal initial spectrum obtained from experimental results.

The three different initial spectra used are presented in Figure 12. The first curve represents the initial spectrum without the interference of any WEC, a Bretschneider spectrum with H_s=2.7 m and T_p= 10.7 s. The third curve represents a hypothetical spectrum resulting from the experimental measurements of spectrum shape with the wave device array in place and as shown in Figure 11. The other spectrum (2) has the initial Bretschneider spectrum shape but with the same significant wave height reduction as the measured spectra, corresponding to the previous curve.

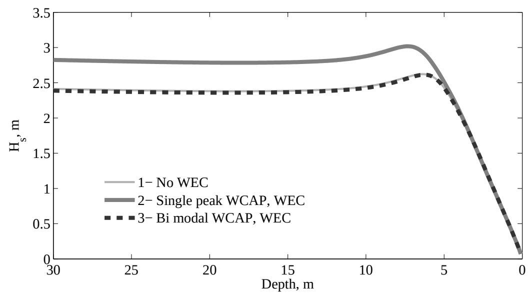

Figure 13: The evolution of the H_s for different water depths. **1-** No WEC, original incident spectrum.**2-** With WEC array originating a single peak wave spectrum, **3-** WEC array with bi-modal initial spectrum obtained from experimental results.

In Figure 13 the H_s evolution is presented for the three different spectra considered. As expected the reduction of H_s by the WEC array is noticeable in all the domain of the problem, including the wave breaking height. Comparing the two different methods for the array representation, the differences in H_s evolution are not very significant when compared with the Figure 3 from the initial study done with the optimal WEC.

The same type of results are verified for the spectral evolution of the waves to the shoreline, Figure 15. In Figure 14 the spectrum of the bi-modal peak from the experiments is shown. The important feature of higher energy in higher frequencies seen in the optimal case presented before, is not completely seen here. As the energy levels at high frequencies noted in deep waters is not very high. This will reduce the influence of the transported energy and also of the dissipation processes. Only when in nearshore waters, depth less than 7 m, a peak at high frequency is seen originated by the wave-wave interaction processes (TRIADS). Figure 15 makes a comparison between the two spectral evolutions for the to WEC array modeling types. The differences however now are not as large as for the idealised case presented in Section 2.

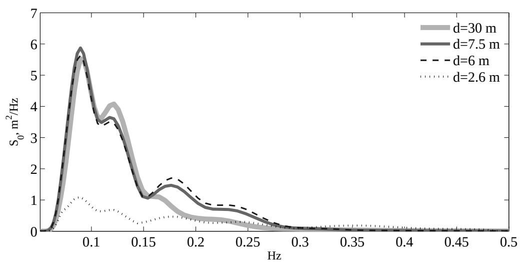

Figure 14: The evolution of the wave spectrum with WEC array defined by the bi-modal case, correspondent to curve 3 of Figure 12

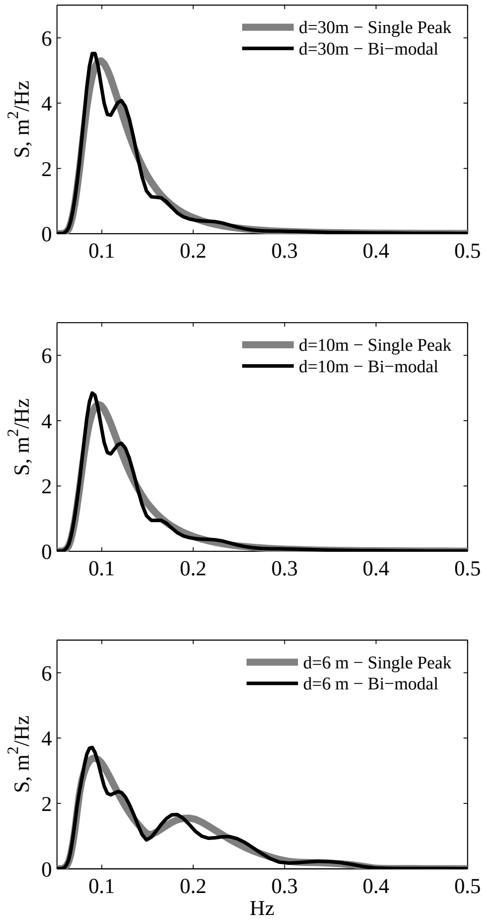

Figure 15: The evolution of the wave spectrum WEC interaction from 12: **1-** With WEC array originating a single peak wave spectrum, **2-** WEC array with bi-modal. For 30, 6 and 2.6 m water depths.

5 Conclusions

In most of the published studies addressing the environmental impact of wave energy converters, devices are represented using uniform energy reduction across the frequency range of the incident waves. Although this corresponds to the average output from wave devices over a period of time, the shape of the incoming wave spectrum is maintained. Here, the influence of frequency-dependent energy extraction on shoreline wave heights is investigated. Modification of an incident Bretschneider spectrum by a wave device tuned to the peak frequency of the spectrum results in a bi-modal spectrum. Comparison is drawn to a single peaked spectrum after equivalent energy extraction (i.e. representing the same transmission coefficient defined in terms of significant wave height reduction). Energy extraction from near the peak of the wave spectrum reduces the energy flux of the wave-field but energy dissipation is reduced between site and shore and this results in a small reduction of breaking wave height. This is a relatively small reduction but may still be important when aspects such as beach erosion are investigated, not only in terms of wave-induced erosion but also due to the influence on other coastal processes such as longshore currents. Throughout this numerical study default values have been employed for energy dissipation coefficients (e.g. whitecapping, bed friction, TRIADS). Since these processes are sensitive to wave frequency, the influence of these parameters requires further study.

An idealised energy extraction model has been employed based on the power capture of a simple spring-mass-damper. In reality these characteristics are not expected to occur and energy extraction would typically be lower except in relatively low energy sea-states. To improve the device representation, a short series of experimental measurements are also presented. Comparisons are drawn between irregular wave measurements up- and down-wave of single and double lines of five heaving devices. Two main regions in the wave spectrum were identified as the place where the main changes across an array of WEC's take place: frequencies around 0.1 Hz, corresponding to the spectrum peak, and 0.15 Hz, close to the natural frequency of the devices. These initial results leave some good indication for future studies. However, experimental tests reported so far are somewhat limited and further tests are required in a range of incident wave conditions, and also using different power configurations, as the H_s reductions is dependent in not a linear fashion with the rated power of the devices. Similar propagation models to the optimal model were used to simulate nearshore conditions. Since measurements are preliminary at this stage only a single spectrum is considered. For these cases, energy extraction is relatively small and so limited change of breaking wave height is predicted although spectral modifications are observed.

Acknowledgements

The first author is a PhD student supported by the EPSRC Supergen Marine II Doctoral Training Programme. The second author is also grateful for the financial support provided by the NWDA Joule Centre for Energy Research. Discussions with Dr Matt Folley of Queens University Belfast and Dr Frank Allison of UMIP are also appreciated.

References

[1] J. Falnes and K. Budal. Wave-power absorption by parallel rows of interacting oscillating bodies. *Applied Ocean Research*, 4(4):194–207, 1982.

[2] D.L. Millar, H.C.M. Smith, and D.E. Reeve. Modelling analysis of the sensitivity of shoreline change to a wave farm. *Ocean Engineering*, 34(5-6):884 – 901, 2007.

[3] H.C.M. Smith, D. L. Millar, and D. E. Reeve. Generalisation of wave farm impact assessment on inshore wave climate. In *Proc. of 7th European Wave and Tidal Energy Conference*, 2007.

[4] V. Venugopal and G.H. Smith. Wave climate investigation for an array of wave power devices. In *Proc. of 7th European Wave and Tidal Energy Conference*, 2007.

[5] C. Vidal, F.J. Mendez, G. Diaz, and L. Legaz. Impact of santoa wec installation on the littoral processes. In *Proc. of 7th European Wave and Tidal Energy Conference*, 2007.

[6] L. Mendes, A. Palha, C. J. Fortes A., Brito-Melo, and A. Sarmento. Analysis of the impact of a pilot zone for wave energy conversion offshore portugal. In *Proc. of 18th International Offshore and Polar Engineering Conference*, pages 401–408. International Society of Offshore and Polar Engineering Conference, July 2008.

[7] TeamSwan. *SWAN users manual*. University of Delft, 1 edition, 2007.

[8] N. Booij, R.C. Ris, and L.H. Holthuijsen. A third generation wave model for coastal regions; part i: model description and validation. *J. of Geophysical Res*, 104:7649–7666, 1999.

[9] K. Hasselman, T. P. Barnett, E. Bouws, D. E. Carlson, and P. Hasselmann. Measurements of wind-wave growth and swell decay during the joint north sea wave project (jonswap). *Deutsche Hydrographische Zeitschrift*, 8, 1973.

[10] K. Hasselmann. On the spectral dissipation of ocean waves due to white capping. *Boundary-Layer Meteorology*, 6:107–127, 1974.

[11] J.A. Battjes and J.P.F.M. Janssen. Energy loss and set-up due to breaking of random waves. In *Proc. 16th Int. Conf. Coastal Engineering*, 1978.

[12] Y. Eldeberky. *Nonlinear transformation of wave spectra in the nearshore zone.* PhD thesis, Department of Civil Engineering, Delft University of Technology, 1996.

[13] L. H. Holthuijsen. *Waves in oceanic and coastal waters*. Cambrige University Press, 1st edition, 2007.

[14] J. Falnes. *Ocean Waves and Oscillating Systems*. Cambrige University Press, 1st edition, 2002.

[15] M. Folley and T.J. Whittaker. Representation of wave energy convertrs in spatial wave models. Technical report, Queens University Belfast report n. QUB 080402, 2008.

[16] T. Stallard, P. K. Stansby, and A. Williamson. An experimental study of closely spaced point absorber arrays. In *Proc. of the Eighteenth International Offshore and Polar Engineering Conference ,Vancouver, BC, Canada, July 6-11*, pages 417–424, 2008.

[17] S. Weller, T. Stallard, and P.K. Stansby. Experimental measurements of irregular wave interaction factors in closely spaced arrays. In *Proc. of the 8th European Wave and Tidal Energy Conference, Uppsala, Sweden*, 2009.

[18] D. Rogers and G. Bolton King. *Wave generation using Ocean and wave*. Edinburgh Designs Ltd, 3.62 1997.